Semaphorin3D regulates invasion of cardiac neural crest cells into the primary heart field

Mariko Sato [a], Huai-Jen Tsai [b], H. Joseph Yost [a,*]

[a] *Huntsman Cancer Institute, Center for Children, Departments of Oncological Sciences and Pediatrics, University of Utah, 2000 Circle of Hope #4280, Salt Lake City, UT 84112, USA*
[b] *Institute of Molecular and Cellular Biology, National Taiwan University, Taipei, Taiwan*

Abstract

The primary heart field in all vertebrates is thought to be derived exclusively from lateral plate mesoderm (LPM), which gives rise to a cardiac tube shortly after gastrulation. The heart tube then begins looping and additional cells are added from other embryonic regions, including the secondary heart field, cardiac neural crest and the proepicardial organ. Here we show in zebrafish that neural crest cells invade and contribute *cardiac myosin light chain2 (cmlc2)*-positive cardiomyocytes to the primary heart field. Knockdown of *semaphorin3D*, which is expressed in the neural crest but apparently not in LPM, reduces the size of the primary heart field and the number of cardiomyocytes in the primary heart field by 20% before formation of the primary heart tube. *Sema3D* morphants have subsequent complex congenital heart defects, including hypertrophic cardiomyocytes, decreased ventricular size and defects in trabeculation and in atrioventricular (AV) valve development. *Neuropilin1A*, a semaphorin receptor, is expressed in LPM but apparently not in the neural crest, and *nrp1A* morphants have cardiac development defects. We propose that a population of *sema3D*-dependent neural crest cells follow a novel migratory pathway, perhaps toward *nrp1A*-expressing LPM, and serve as an important early source of cardiomyocytes in the primary heart field.
© 2006 Elsevier Inc. All rights reserved.

Keywords: Heart development; Neural crest; Zebrafish; Cardiomyocyte; Cardiogenesis; *semaphorin3D*; *cmlc2*

Introduction

Cardiomyocytes, the major structural and functional cell population in the heart, originate from cardiac progenitor cells in bilaterally separate "primary heart fields" of the anterior lateral plate mesoderm (LPM) in all vertebrates. These fields, traditionally known as the cardiac crescent, are established during gastrulation by inductive interactions (Harvey, 2002) and migrate toward the embryonic midline to fuse into the heart tube. Until recently, the primary heart field was thought to be the sole source of cardiomyocytes. However, there are now two other known sources that contribute cardiomyocytes later in development, after cardiac tube formation: secondary heart field in chick and mouse (Eisenberg and Markwald, 2004; Kelly and Buckingham, 2002; Kelly et al., 2001; Mjaatvedt et al., 2001;

Waldo et al., 2001) and neural crest in zebrafish (Li et al., 2003; Sato and Yost, 2003). Our previous fate mapping showed that a population of the neural crest contributes to cardiomyocytes in the atrium, atrioventricular junction, and the ventricle in zebrafish (Sato and Yost, 2003). By extensive fate map analyses, we and others have shown that zebrafish cardiac neural crest cells are incorporated into cardiac structures and express myocardial markers by the time the heart is fully formed and functional at 36 hours post-fertilization (hpf) (Li et al., 2003; Sato and Yost, 2003). However, the developmental timing, the migratory route and the molecular signals that control neural crest arrival in the developing heart are unknown.

In zebrafish, cardiomyocytes first differentiate from the precardiac LPM at the 13–14 somite stages (SS) at approximately 15 hpf, detected by myocardial markers such as *cmlc2* (cardiac myosin light chain 2) and *vmhc* (ventricular myosin heavy chain) in a bilateral expression pattern (Glickman and Yelon, 2002; Yelon and Stainier, 2002; Yelon et al.,

* Corresponding author. Fax: +1 801 585 5470.
E-mail address: joseph.yost@hci.utah.edu (H.J. Yost).

1999). The myocardial precursors merge posteriorly to form a horseshoe-shaped structure at 19 hpf (20 SS). By 19.5 hpf (19–20 SS), anterior myocardial precursors migrate medially, the horseshoe transforms into a doughnut shape/cone, which telescopes out to form a tube (Stainier, 2001). By 22 hpf (26 SS), the primary heart tube has elongated and changed its orientation so that it is positioned with the cranial part of the tube toward the left side of the embryo. After contraction begins, heart development is regulated not only by molecular and cellular mechanisms but also by circulation of fluid (Hove et al., 2003). It is known that endocardial cushion formation, which leads atrioventricular valve formation, is dependent on both myocardial patterning and intracardiac hemodynamics in zebrafish (Bartman et al., 2004; Hove et al., 2003). Trabeculation occurs between 2 and 4 dpf; however, the mechanism is not well understood.

Semaphorins represent a family of membrane bound and secreted factors characterized by a conserved semaphorin domain (Kolodkin et al., 1993; Luo et al., 1993). Semaphorins are expressed in the central nervous system, where function has been extensively analyzed (Luo et al., 1995). Semaphorins were originally identified as inhibitory axon guidance cues, although recent studies have shown that some can be attractive (Kolodkin et al., 1993; Mark et al., 1997; Raper, 2000). Subsequently, semaphorins have been shown to be important regulators of diverse biological processes, including neural crest development (Yu and Moens, 2005).

Among semaphorin family genes, Class3 semaphorin is known to function in neural crest migration. In chick, *semaphorin3A* signaling participates in the molecular mechanisms that determine the segmental pattern of both trunk and hindbrain crest cell migration (Eickholt et al., 1999). Simultaneously, *neuropilin-1* was identified as a candidate receptor that might mediate this response. In mice, *semaphorin3C* deficient mice die immediately after birth, due to aortic arch malformation and septation defects in the outflow tract of the heart. This suggests that *semaphorin3C* promotes the migration of cardiac neural crest cells into the proximal outflow tract (Feiner et al., 2001). *PlexinA2* is a member of a large family of receptors that recognize secreted semaphorin signaling molecules and is expressed by migrating and post-migratory cardiac neural crest cells. It also plays a functional role in cardiac neural crest migration by acting as a co-receptor for Class3 semaphorin signaling molecules in mice (Brown et al., 2001).

Semaphorin3D (*sema3D*) is a secreted semaphorin expressed during development of the nervous system and the neural crest in zebrafish (Halloran et al., 1999). Morpholino knockdown studies showed that *sema3D* is important in retinal axon guidance (Liu et al., 2004) as well as the correct formation of early axon pathways (Wolman et al., 2004). Here we report that *sema3D* signaling is also important in the development of neural-crest-derived cardiomyocytes. Knockdown of *sema3D* function results in defects in myocardial development within the primary heart field just before the cone telescopes to form a cardiac tube. By transplanting lineage-
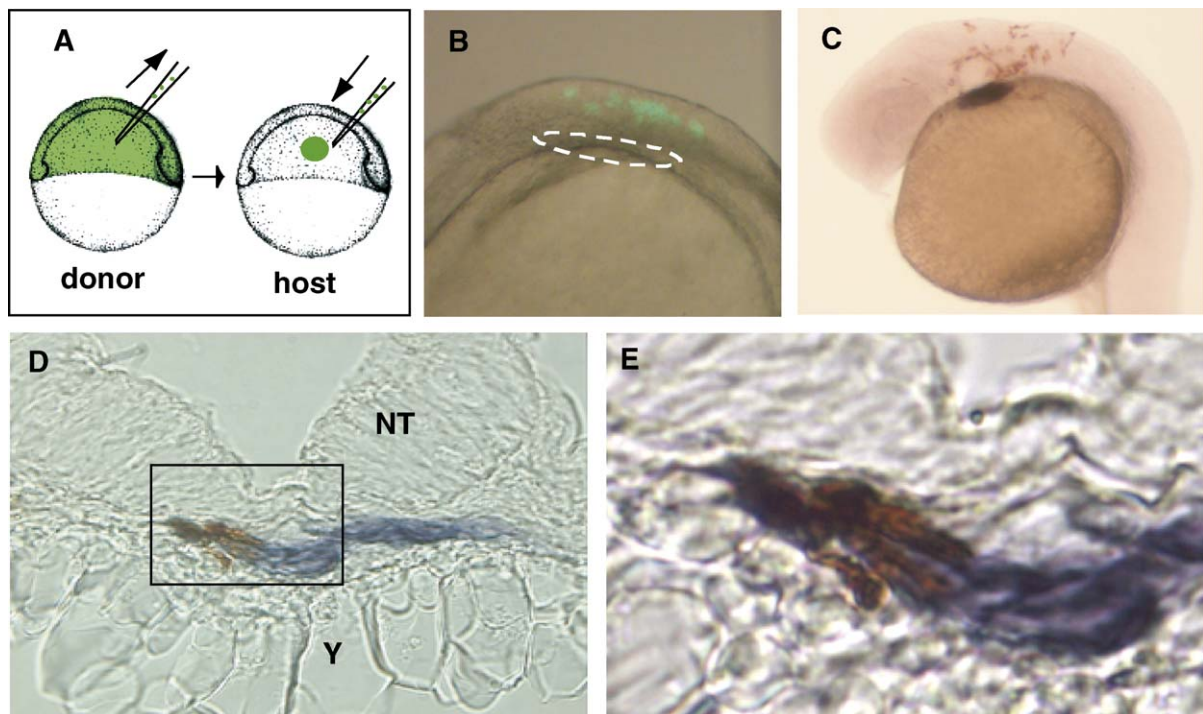

Fig. 1. Neural crest cells migrate to the primary heart field and express *cmlc2*. (A) Transplantation strategy. At the shield stage, 10–50 prospective neural crest cells were transplanted from fluorescein dextran donors into the orthotopic region of hosts. (B) 8 SS embryo, DIC and epi-fluorescent (lateral view, anterior at left, dorsal at top). Lineage-labeled cells (green) were in neural crest and neural tube at hindbrain level, but not in anterior LPM (white circle). (C) 26 SS embryo, lineage-labeled cells (anti-fluorescein antibody, brown) and cardiomyocytes (*cmlc2*, purple) were detected. (D) Transverse section through the primary heart field of 26 SS embryo with lineage-labeled neural crest cells (brown) expressing *cmlc2* (purple). NT = neural tube, Y = yolk. (E) Magnified image of box in panel D.

labeled cells, we found neural crest cells express *cmlc2* within the primary heart field. These results implicate for the first time a role for neural crest cells in primary heart field development and suggest that an early wave of neural crest cells invade the primary heart field and contribute precardiac mesodermal cells to before the heart tube forms.

Materials and methods

Zebrafish maintenance

Zebrafish, *Danio rerio*, were maintained at 28.5°C on a 14-hour/10-hour light/dark cycle. Embryos were collected from natural spawning and cultured and staged by developmental time and morphological criteria (Westerfield, 1994). *Cardiac myosin light chain 2 (cmlc2)-gfp* transgenic fish were kindly provided by H. Tsai (Huang et al., 2003; Shu et al., 2003).

Cell transplantation

At the one-cell stage, wild-type donors were injected with fluorescein dextran (10,000MW, Molecular Probes), a fixable cell lineage tracer. Both donor and host embryos at shield stage were dechorionated and positioned into wells in an agarose plate. Approximately 10–50 donor cells in the future neural crest region, identified with respect to the shield, were transplanted into the homotypic position of an age-matched host embryo (Sato and Yost, 2003). This position does not overlap with the ventral and equatorial mesodermal region that has previously been fate-mapped to give rise to the heart tube (Keegan et al., 2005; Stainier et al., 1993). At 8 SS, embryos with lineage-labeled cells transplanted into the neural crest and the neural tube, but not into the anterior LPM, were selected for further analysis.

In situ hybridization, immunohistochemistry and cartilage staining

Whole-mount *in situ* hybridization was performed using digoxigenin-labeled antisense RNA probes: *cmlc2* (Yelon et al., 1999); *crestin* (Rubinstein et al., 2000); *foxd3* (Odenthal and Nusslein-Volhard, 1998); *rag1* (Willett et al., 1997); *semaphorin3D* (Halloran et al., 1999); *AP2* (Hilger-Eversheim et al., 2000); *neuropilin1A* (Lee et al., 2002). Whole-mount immunohistochemistry was carried out with POD conjugated anti-fluorescein antibody (Molecular probes). For cartilage staining, alcian blue staining was performed as previously described (Neuhauss et al., 1996).

Morpholino oligonucleotides

The sequences of *sema3D* morpholinos (kindly provided by M. Halloran) are as follows: *sema3D*-augMO (blocking start site): 5′-CATGATGGACGAGGA-GATTTCTGCA-3′, controlMO: 5′- CATCATGCACGAGGAGATATCTCCA-3′ (Liu et al., 2004), *sema3D*-spMO (targeting at the site between intron 4 and

exon 5): 5′-CACATTCAGTCTGCAGCAAGAGAAA-3′. The *Nrp1A* morpholino is 5′-GAATCCTGGAGTTCGGAGTGCGGAA-3′ and the control morpholino is 5′- GATTCCAGGAGTTCGGACTGCCGAA-3′.
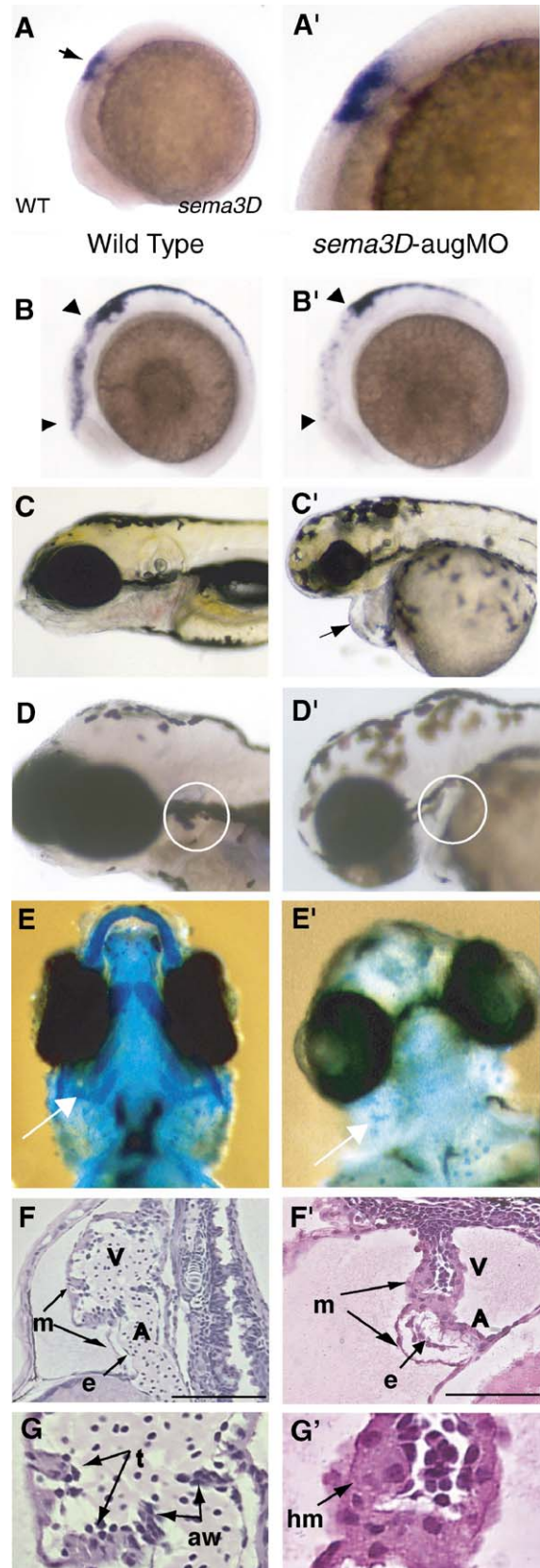

Fig. 2. *sema3D*-aug morphants have cardiac neural crest defects. (A, A′) At 8 SS, *sema3D* RNA is expressed in rhombomere 3–5 and in neural crest (black arrow). Anterior left, dorsal up. (B–F′) Phenotypic analyses of wild-type (B–F) and *sema3D*-augMO morphants (B′–F′). Morphants had reduced crestin expression in cranial crest (8SS, arrowheads, B and B′), pericardiac edema (4 dpf, arrow c′) and shortened neck indicative of pharyngeal arch defects, decreased *rag1* expression in the thymus (white circle, D′), and defective facial and pharyngeal cartilage development (white arrow, alcian blue staining, ventral view, E′). These phenotypes are indicative of neural crest defects. (F, F′) *Sema3D* morphants have dysmorphic hearts with smaller ventricle (V), smaller atrium (A) and thickened myocardium (m). Endocardium was present (e), but AV valve and trabeculation were absent (4 dpf, lateral section, H&E stain, 100 μm scale bar). (G, G′) Magnified pictures of F and F′, respectively. Trabeculation (t) and AV valve formation (avv) observed in wild-type embryo was not found in morphant. In morphant, hypertrophic cardiomyocytes (hm) were observed.

Histological sections

Two to four dpf larvae were fixed in 4% paraformaldehyde overnight and serially dehydrated. Using Immuno-Bed Kit (Polysciences, Inc. PA), embryos were transferred to infiltrate solution overnight, positioned and embedded into the wells under the dissection microscope, as described by Finkelstein et al. (1999). A glass knife microtome was used to cut 5-µm sections, which were collected on glass slides and stained with hematoxylin and eosin. Cryostat sections (10 µm thick) were also performed as described in Zebrafish Book (Westerfield, 1994).

cmlc2 expression analyses

To visualize *cmlc2* expression, embryos were mounted in glycerol. Dorsal views were taken using Nikon COOLPIX digital camera and processed using Adobe Photoshop software. Scion Imaging Software (www.Scioncorp.com) was used to measure the area of *cmlc2* expression.

Cell count

Embryos were dissociated at 26 hpf using the mechanical dissociation method previously described (Shu et al., 2003), and GFP-positive cells were counted using a Leica DMRA microscope.

Results

Cardiac neural crest cells contribute to the primary heart tube

Our previous fate-mapping showed that a population of the neural crest contributes to cardiomyocytes in the atrium, atrioventricular junction and the ventricle in zebrafish by the time heartbeat begins (Sato and Yost, 2003). However, the

developmental timing, the migratory route and molecular signals that control neural crest arrival in the developing heart are unknown. In order to assess the timing and migratory pathway, we fluorescently labeled neural crest cells by microinjection and cell transplantation (Fig. 1A). At the beginning of neural crest migration (8 somite stage, 8 SS), embryos that had labeled cells in the neural crest but not in LPM were selected (Fig. 1B) and allowed to develop to either 22 SS ($n = 30$) or 26 SS ($n = 16$). Lineage-labeled cells were detected by immunohistochemistry with anti-fluorescein antibody and cardiomyocytes were detected by *in situ* hybridization with *cmlc2* (Fig. 1C). Cryostat sectioning revealed 6 of 46 embryos (2 at 22 SS, 4 at 26 SS) with lineage-labeled neural crest cells that had invaded the primary heart field and had converted to *cmlc2*-expressing myocardial precursors (Figs. 1D and E). In zebrafish, starting at about 20 SS (19 hpf), bilateral myocardial primary heart field precursors migrate medially to fuse at the midline. In the next few hours (by 26 SS), the field telescopes out, in a cone shape, to form a tube. The ventricular end of the heart tube assembles first followed by the atrial end (Stainier, 2001; Yelon et al., 1999). Our results indicate that lineage-labeled neural crest cells express *cmlc2* in the primary heart field by the time it is forming a cone-shaped tube.

Sema3D knockdown alters cardiac neural crest development

The molecular regulation of cardiac neural crest is poorly understood. *Class3 semaphorins* have general roles in neural crest migration in chick and zebrafish (Halloran and Berndt,
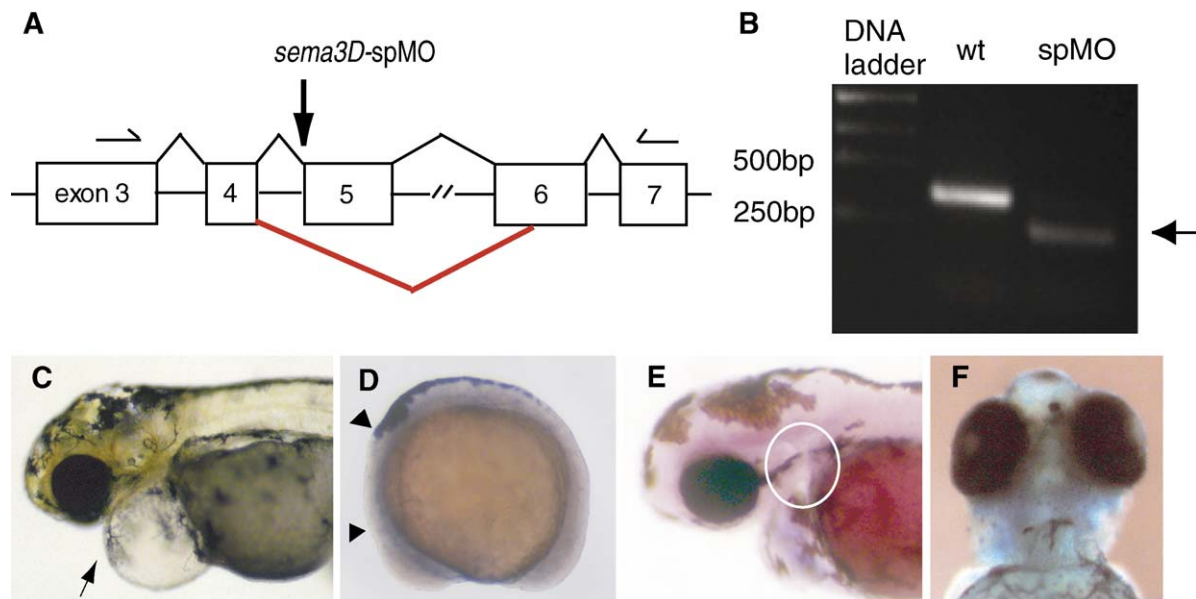

Fig. 3. *sema3D*-splice blocking morpholino knocks down *sema3D* mRNA and phenocopies *sema3D*-augMO. (A) Genomic structure of *sema3D* gene (GenBank #NM 131048), exons (boxes, not to scale). Splice donor site between 4th intron and 5th exon (5th exon codes amino acids in sema domain) was targeted by *sema3D*-spMO. The red line indicates the major splice variant observed following spMO injection. Primers used for RT-PCR analysis in B are shown as arrows (forward 5′-CCA GAC AAC ATC AAT AAA CAC CCC-3′, reverse 5′-TTG CCC AGG AAA TCA GAC GC-3′). (B) The single fragment (exons 3–7, 350bp) amplified from wild-type RNA was diminished by *sema3D*-spMO and replaced by a smaller fragment (arrow, 230bp). Sequencing revealed that *sema3D*-spMO caused utilization of cryptic splice sites, deleting exon 5 and part of exon 6, removing amino acids 129 through 168 (nucleotides 656–775 in *sema3D* mRNA), deleting the essential *sema* domain. *Sema3D*-spMO morphants had the same phenotypes as *sema3D*-augMO, including severe pericardiac edema (C, arrow, 4 dpf), reduction of *crestin* expression in cranial neural crest (D, arrowheads, 8 SS), reduction of *rag1* expression in the thymus (E, white circle, 4 dpf) and loss of facial and pharyngeal cartilages (F, Alcian blue staining, 4 dpf).

2003; Osborne et al., 2005; Yu et al., 2004) and roles pertinent to cardiac neural crest development in mice (Brown et al., 2001; Feiner et al., 2001). To further investigate *Class3 semaphorin* signaling in cardiac development and to assess whether *sema3D* might serve as a tool with which to manipulate precardiac neural crest, *sema3D* expression and function were analyzed in zebrafish. *Sema3D* was expressed in the cranial neural crest at the level of rhombomeres 3, 4 and 5 at 12 hpf (Figs. 2A and A′), coinciding with a subset of cardiac neural crest that we had previously mapped in zebrafish (Sato and Yost, 2003). Later, *sema3D* was expressed in post-otic migrating neural crest (24 hpf) and in a subset of pharyngeal arches (48 and 72 hpf, MS and HJY, data not shown) (Halloran et al., 1999). In contrast to its neural crest expression, *sema3D* was not detected in the developing heart from 8 SS through 72 hpf. This indicates that *sema3D* is expressed in cardiac neural crest before it migrates to the heart-forming region, and that *sema3D* is not apparently expressed in the lateral mesoderm-derived primary heart primordium *per se*. Thus, inhibition of *sema3D* function provides a test of the roles of cardiac neural crest without directly affecting precardiac lineages derived from lateral mesoderm.

Heart defects are striking in *sema3D-aug* morphants. At 4 dpf, morphants had a small and dysmorphic ventricle and atria, hypertrophic cardiomyocytes in the ventricle, reduced trabeculation and defective AV valve formation (Figs. 2F′, G′ and Supplementary Fig. 1). Thus, loss of *sema3D*-dependent neural crest cells has profound impact on ventricle formation, trabeculation and AV valve development, leading to complex congenital heart defects.

Sema3D-aug morphants displayed several molecular and morphological phenotypes that are hallmarks of neural crest deficiency. The pan-neural crest marker *crestin* was severely reduced in cranial neural crest in morphants (Fig. 2B′). At 4 dpf, *sema3D* morphants had short necks and pericardiac edema (Fig. 2C′), reduction in the thymus marker *rag1* (Fig. 2D′) and facial and pharyngeal cartilage defects (Fig. 2E′). The pharyngeal phenotypes were consistent with a defect in neural crest contribution to pharyngeal arches that occurs between 18 and 24 hpf (Miller et al., 2000; Schilling and Kimmel, 1994). To verify the specificity of *sema3D*-aug MO function, we tested a second morpholino (*sema3D*-spMO), which targeted the splice donor site at the junction of intron 4 and exon 5 (Fig. 3A). Splice site-blocking MO have been used successfully to disrupt splicing of specific transcripts in zebrafish embryos and, advantageously, the efficacy of splice site-blocking MOs can be measured by RT-PCR (Draper et al., 2001). Using primers in exons 3 and 7 of *sema3D*, RT-PCR analysis of total RNA extracted from embryos at 2 dpf indicated that injecting *sema3D*-spMO blocked normal splicing (Fig. 3B). Aberrant splicing between exons 4 and 6 were confirmed by sequencing RT-PCR products (data not shown). Embryos injected with *sema3D*-spMO showed similar phenotypes to *sema3D*-aug morphants, including heart edema, defects in *crestin* and *rag1* expression and pharyngeal cartilage defects (Figs. 3C–F), suggesting that both morpholinos block *sema3D* function specifically.

To further assess the effects of *sema3D* morpholino on neural crest development, we examined the expression of

foxd3 and *AP2* (Fig. 4). Both *foxd3* and *AP2* were expressed in the cranial neural crest in *sema3D* morphants. However, the expression patterns observed in dorsal views revealed that neural crest migration patterns were disrupted (Figs. 4A′, B′ and C′, D′, respectively). In summary, knockdown of *sema3D*
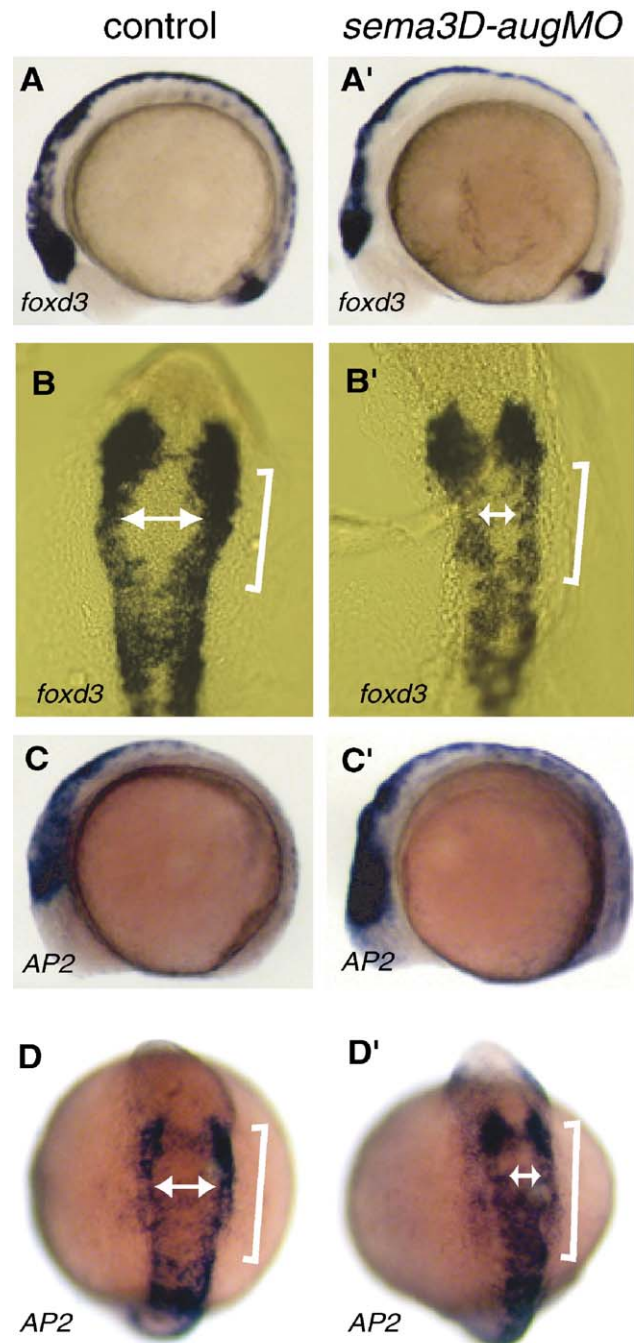

Fig. 4. Migratory defects were observed with *foxd3 and AP2* in *sema3D*-aug morphants. In situ hybridization with *foxd3* (A, A′, B, B′) and *AP2* (C, C′, D, D′). Both markers were expressed including the cranial neural crest at 8 SS. Dorsal views (B, B′, D, D′, cranial up) showed that cells expressing both markers in morphants did not migrate as far as those in wild type, suggesting that migratory pattern was disrupted. Brackets in panels B, B′, D and D′ showed altered pattern of migration. White arrows in panels B, B′, D and D′ indicated the distance of migrating neural crest cells.

results in defects in migrating neural crest as well as in defects in the pharyngeal arch and the thymus, which are considered to be neural crest derivatives.

Neural crest defects lead to defects in cmlc2 expression in the primary heart field

The dysmorphic hearts observed in *sema3D* morphants have hypertrophic cardiomyocytes and lack trabeculation, considered to be indicative of defects in myocardial development. Heart development before 4 dpf was superficially normal, but a molecular analysis revealed early defects in the primary heart field. Consistent with the early contribution of neural crest cells to the primary heart tube (Figs. 1C–E), *cmlc2* expression in the primary heart field was altered in *sema3D*-aug morphants at 19–20 SS, that is before the primary heart tube is formed and elongated (Figs. 5A–C). This precedes the start of circulation and therefore occurs before traditional cardiac neural crest defects in pharyngeal arch and outflow tract would have an opportunity to indirectly impact cardiac development. At 19–20 SS, the primary heart field is a flat sheet of cells (Trinh and Stainier, 2004), so that the dorsal view of *cmlc2* expression allows fairly accurate measurements of the dimensions of the primary heart field. By measuring the outside diameter (O) and inside diameter (I) of the *cmlc2*-labeled primary heart field, we found that the primary heart field was smaller in *sema3D*-aug morphants than in controls, at 19–20 SS (MO: $n = 18$, control: $n = 13$) (Fig. 5C). The area of *cmlc2* expression (S) was calculated using mean values of O and I using the formula $S = (O^2 - I^2) \, 1/4 \, \pi$, assuming *cmlc2* expression pattern was doughnut shaped. The area S in morphant ($2964 \, \mu m^2$) was significantly smaller than S in controls ($4359 \, \mu m^2$) at the 19–20 SS ($P < 0.001$, 95% confidence interval: 633.5, 2156.0). Because the heart field begins to change shape away from a plane at 21–22 SS, the area measurements at subsequent stages are more difficult to interpret. The yolk diameters (Y) in morphants at 19–20 SS ($659.0 \pm 21.2 \, \mu m$) were slightly wider (1–5%) than in controls (627.7 ± 24.0), indicating that the smaller field of *cmlc2* expression in the morphants is not due to a smaller embryo size in morphants.

In a complementary approach to analyze the role of *sema3D* in formation of the primary heart field, we counted cardiomyocytes at 26 hpf using *cmlc2*::EGFP transgenic line that drives EGFP expression specifically in cardiomyocytes (Huang et al., 2003) (Figs. 5D and E). Control embryos had 184 ± 15 ($n = 30$ embryos) cardiomyocytes at 26 hpf, comparable to a previous report (186 ± 19, $n = 16$ at 24 hpf) (Shu et al., 2003). In contrast, *sema3D*-aug morphants had significantly fewer GFP-
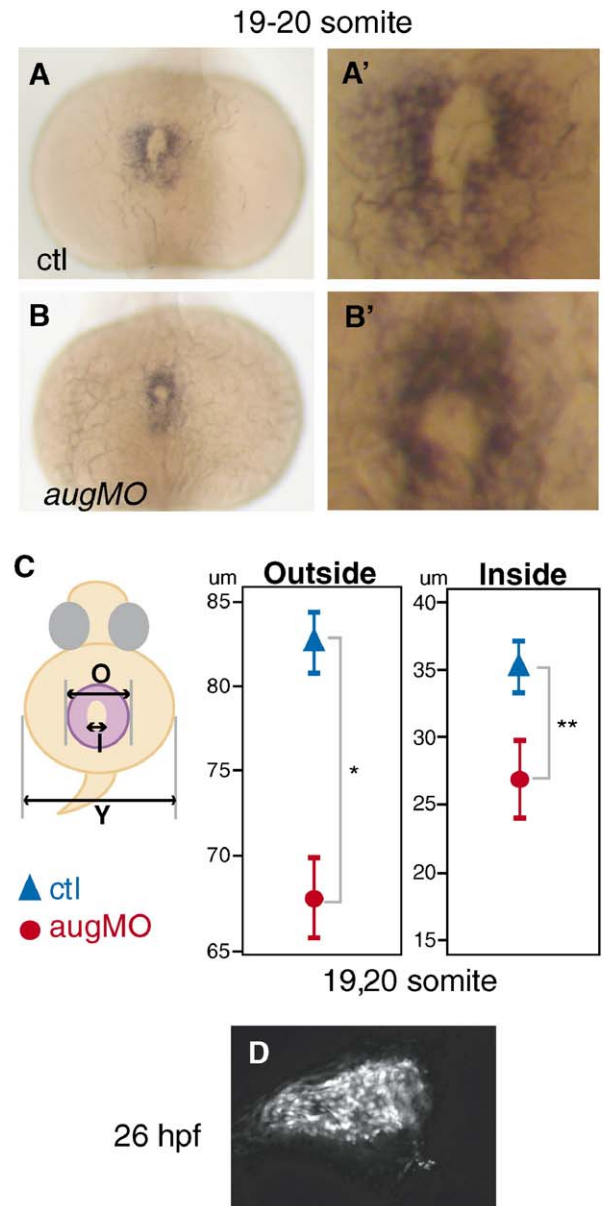

Fig. 5. *sema3D* morphants have fewer cardiomyocytes in the primary heart field. Dorsal views *cmlc2* expression in control (A, A′) and *sema3D* morphants (B, B′). (C) Schematic diagram of inside (I) and outside (O) diameters of *cmlc2* expression (purple) and (Y) yolk diameter. Graphs indicate mean ± one standard deviation of diameters measured (μm) in *sema3D* morphants (red circles, $n = 18$) and controls (blue triangles, $n = 13$). The primary heart field is significantly smaller in *sema3D* morphants (*$P = 0.0002$, **$P = 0.0549$). (D) An image of dissociated *cmlc2-gfp*-positive heart at the 26 hpf, after arrival on neural crest. (E) Count of number of cardiomyocytes from dissociated *cmlc2*::EGFP embryos. y axis is mean number of EGFP-positive cardiomyocytes, bars indicate standard deviation. Control embryos had 184 ± 15 ($n = 30$) cardiomyocytes. Both aug-MO and sp-MO-injected embryos had significantly fewer GFP-positive cardiomyocytes (aug-MO: 145 ± 21, $n = 23$, sp-MO: 154 ± 11, $n = 11$) than control (*$P < 0.0001$).
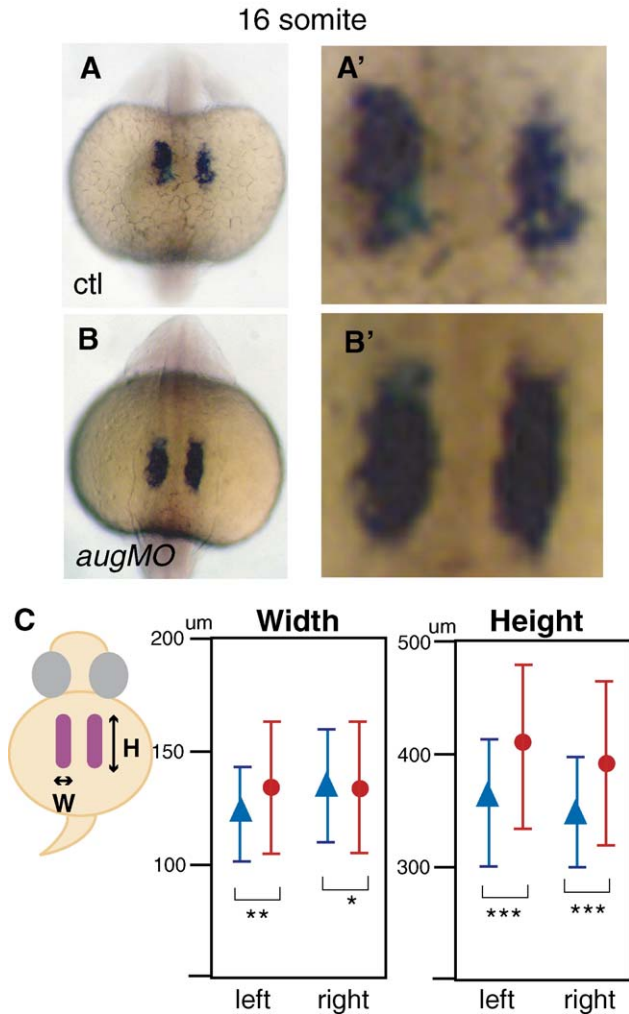
16 somite

Fig. 6. *sema3D* morphants have normal precardiomyocytes in LPM before neural crest arrival and diminished number of cardiomyocytes later. Dorsal views *cmlc2* expression in control (A, A′) and *sema3D*-aug morphants (B, B′) at the 16 SS. Panels A′ and B′ are magnified *cmlc2* expression pattern. (C) Schematic diagram of width (W) along the proximal–distal axis and height (H) along the anterior–posterior axis of *cmlc2* expression (purple). Graphs indicate mean ± one standard deviation of width and height measured (μm) in *sema3D* morphants (red circles, $n = 32$) and controls (blue triangles, $n = 37$). Before the arrival of neural crest cells, the size of the primary heart field in *sema3D* morphants is similar to or slightly larger than the heart field in controls. $*P = 0.624$, $**P = 0.09$, $***P = 0.005$.

positive cardiomyocytes ($145 ± 21$, $n = 23$) than control ($P < 0.0001$) (Fig. 5E). Similar to *sema3D*-aug morphants, *sema3D*-sp MO-injected embryos ($n = 11$) had a decrease in cardiomyocyte number ($154 ± 11$ *cmlc2-gfp*-positive cells) compared to controls ($P < 0.0001$; Fig. 5E). Thus, *sema3D*, expressed in neural crest, is required for the establishment of normal cardiomyocyte cell number in the primary heart field and tube in zebrafish.

Sema3D knockdown does not affect induction of lateral plate mesoderm-derived cardiomyocytes

The model that neural crest contributes cells to the primary heart field predicts that primary heart fields in *sema3D*

morphants and controls should be similar in size before the invasion of cardiac neural crest. To test this model, we examined primary heart fields before the arrival of neural crest, using two early markers of heart development. The expression patterns of *nkx2.5* at 8 SS (MS and HJY, data not shown) and *cmlc2* at 16 SS Figs. 6A, A′ and B, B′) were similar in morphants and controls. This indicates that *sema3D* knockdown does not affect the induction or patterning of the early primary heart field derived from LPM, and suggests that the cardiac defects in sema3D morphants are due to defects in the neural crest-derived component of the primary heart field.

Neuropilin1A morphant phenotypes are similar to those of sema3D morphants

In contrast to *sema3D*, a candidate receptor *neuropilin1A (nrp1A)* is expressed in LPM and apparently not in the neural crest at 8 SS (Fig. 7A). Morpholino knockdown of *nrp1A* results in a range of phenotypes, including pharyngeal arch defects and diminished *rag1* expression (Figs. 7B–C), that are indicative of neural crest defects, similar to those seen in *sema3D* morphants. This suggests that loss-of-function of *nrp1A* in LPM or other targets results in diminished migration of neural crest destined for the cardiac tube but does not directly assess the action of nrp1A on crest. Correspondingly, *nrp1A* morphants have cardiac defects similar to those seen in *sema3D* morphants (Fig. 7D).
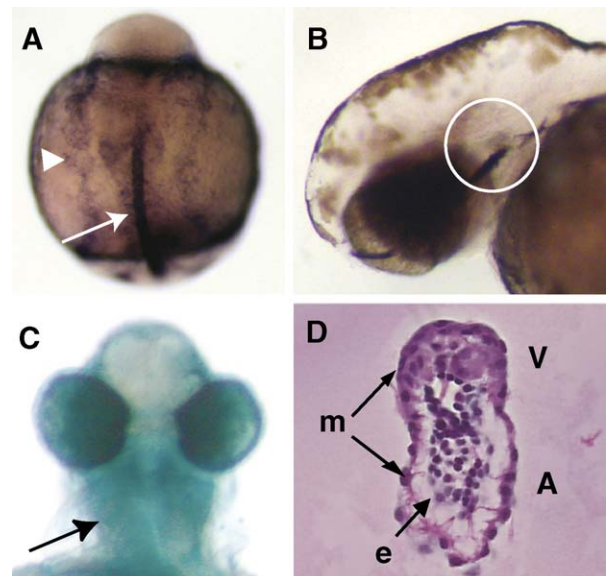

Fig. 7. *neuropilin1A* is expressed in LPM and morphant phenotypes are similar to those of *sema3D* morphants. (A) At 8 SS, *nrp1*A RNA is strongly expressed in LPM (shown in arrowhead) and in the notochord (shown in arrow), not in neural crest. Dorsal view of embryo, cranial to the top. (B) *rag1* expression in the thymus (white circle) was reduced in morphants. (C) Alcian blue staining showed defective facial and pharyngeal cartilage development (arrow, ventral view). (D) *nrp1A* morphants have dysmorphic hearts with smaller ventricle (V), smaller atrium (A) and thickened myocardium (m). Endocardium was present (e) (4 dpf, lateral section, H&E stain).

Discussion

Using transplantations to lineage label neural crest cells and knockdown of *sema3D* in neural crest, we report the surprising finding that neural crest cells migrate directly into the primary heart field just before the tube formation and express *cmlc2*, indicating their transformation into myocardial precursors/ cardiomyocytes. In our previous fate mapping studies, it was striking that neural crest in zebrafish makes a larger contribution to cardiac development than is known in other vertebrates and differentiate into cardiomyocytes distributed throughout the heart, including atrium, atrioventricular cushion, ventricle and bulbus arteriosus (Sato and Yost, 2003). The mechanisms by which neural crest contributed to heart development were unknown. Here we propose that neural crest cells directly participate in the formation of the primary heart field. Loss of neural crest contribution, as seen in *sema3D* morphants, results in a significant reduction in the number of cardiomyocytes in primary heart field at 19–20 SS, diminished numbers of cardiomyocytes at 26 hpf after the cardiac tube has formed, and subsequent defects in heart development.

Sema3D is expressed exclusively in the neural crest at 8 SS, coincident with a subset of neural crest cells that we have previously fate-mapped to contribute to heart development (Sato and Yost, 2003), and does not appear to be expressed in LPM or heart primordium at any stage of early development. As with any expression analysis, it is possible that *sema3D* is expressed in LPM at levels below the detection limits of in situ hybridization. However, knockdown of *sema3D* function perturbs early neural crest development without affecting LPM-derived precardiac mesoderm patterning at 8 SS and 16 SS (as indicated by *nkx2.5* and *cmlc2* expression). This argues against two alternative possibilities: *sema3D* expressed at subdetectable levels in LPM or other tissues directly control LPM patterning or *sema3D* expressed in pre-migratory neural crest reaches LPM to control its early patterning. We estimate that neural crest arrival in the primary heart field occurs between 16 and 20 SS, based on the normal size of the cardiac field at 16SS and altered size by 20SS. In contrast to normal precardiac mesoderm patterning before 16 SS in *sema3D* morphants, pre-migratory neural crest is specified but does not migrate normally in *sema3D* morphants. Together, these observations indicate that *sema3D* morpholino injection is an effective approach to prevent migration of cardiac neural crest cells into the primary heart field. It is striking that *sema3D* knockdown diminishes the migration of neural crest cells in a rostral–caudal zone that is broader than the zone of neural crest cells that express *sema3D* mRNA. Because some semaphorins are secreted molecules, one explanation for the effects of *sema3D* knockdown beyond the range of *sema3D* expression in neural crest is that neural crest migration is dependent on paracrine signaling by *sema3D*. To further explore the mechanism by which *sema3D* knockdown alters neural crest development, we performed TUNEL assay on both 8 SS and 24 hpf embryos and found an increased number of apoptotic cells within the non-migratory neural crest population at 24 hpf (MS and HJY, data not shown). From these observations, the most parsimonious explanation for neural crest and primary heart field defects in *sema3D* morphants is that sema3D allows the migration of a wide rostral–caudal zone of previously specified neural crest cells. In the absence of *sema3D*-dependent migration, neural crest cells eventually succumb to apoptosis in their pre-migratory positions instead of contributing to approximately 20% of the primary heart field.

The interaction between *sema3D*-expressing neural crest and primary heart field may be dependent on semaphorin–neuropilin signaling. In zebrafish, there are four neuropilins, *nrp-1A*, *1B*, *2A* and *2B* (Bovenkamp et al., 2004; Lee et al., 2002). Among them, *nrp-1A* and *nrp-2B* are known to function as receptors of *sema3D* in axon guidance (Wolman et al., 2004). In addition to later vascular expression (Lee et al., 2002), *Nrp-1A* is expressed in LPM toward which neural crest emigrates (Fig. 7A) when the neural crest arrive at the primary heart field but does not appear to be expressed in neural crest. Strikingly, *nrp1A* morphants displayed phenotypes indicative of neural crest defects similar to those seen in *sema3D* morphants, such as thymus and pharyngeal arch defects as well as heart defects (Fig. 7) in addition to later-onset vascular defects reported by Lee et al. (Bovenkamp et al., 2004; Lee et al., 2002). An intriguing model in which *sema3D* in neural crest and *nrp1A* in LPM interact in order to control migration of neural crest to the primary heart field awaits further analysis.

The direct contribution of neural crest cells to the primary heart field has not been described in any vertebrate. It is possible that early contributions of neural crest reported here in zebrafish have been overlooked in chick and mice due to technical constraints, or that this early migratory pathway in zebrafish has been evolutionarily usurped in air-breathing vertebrates due to requirements to generate significant left–right asymmetries in the outflow tract. In chick and mice, cardiac neural crest is thought to first migrate into pharyngeal arches and thence migrate into the outflow tract of the heart, long after the heart tube has formed and begun looping (Chan et al., 2004; Epstein et al., 2000; Kirby and Waldo, 1990, 1995). A similar late migratory path also occurs in zebrafish. Lineage labeling study performed by Schilling et al. found that labeled neural crest cells contributed to the hyoid arch primordium at 24 hpf (Schilling and Kimmel, 1994), and *endothelin-1* and *dlx2* are expressed in pharyngeal mesenchymal cluster of cells at 18–20 hpf (Aki-menko et al., 1994; Kimmel et al., 2001; Miller et al., 2000). These results indicate that neural crest in zebrafish contributes to pharyngeal archs between 18 and 24 hpf, analogous to cardiac neural crest in chick and mice. After the initiation of heart beat, *sema3D* morphants have distinct cardiac defects, including hypertrophic cardiomyocytes and a lack of ventricular trabeculation. Given the breadth of the neural crest defects in *sema3D* morphants, it is likely that some of these late-onset cardiac defects are due to secondary effects of pharyngeal arch and circulatory defects that might alter intracardiac hemodynamics (Bartman et al., 2004; Hove et al., 2003).

Analyses of several zebrafish heart mutants have revealed molecular mechanisms that regulate formation of the primary heart field and subsequent heart development (Chen et al., 1996; Reiter et al., 1999; Stainier, 2001; Stainier et al., 1996, p. 524).

Here we utilize *sema3D* morphants to show that defects in neural crest can give rise to defects in primary heart field development. These findings suggest that it would be judicious to ask whether mutants that have defects in primary heart field formation have defects in neural crest development, not just defects in endoderm or LPM. Previous cardiac fate maps of primary heart field in zebrafish (Kimmel et al., 1990; Stainier et al., 1993) need to be revised to include the neural crest.

Acknowledgments

Appendix A. Supplementary data

Supplementary data associated with this article can be found, in the online version, at doi:10.1016/j.ydbio.2006.05.033.

References

Akimenko, M.A., Ekker, M., Wegner, J., Lin, W., Westerfield, M., 1994. Combinatorial expression of three zebrafish genes related to distal-less: part of a homeobox gene code for the head. J. Neurosci. 14, 3475–3486.

Bartman, T., Walsh, E.C., Wen, K.K., McKane, M., Ren, J., Alexander, J., Rubenstein, P.A., Stainier, D.Y., 2004. Early myocardial function affects endocardial cushion development in zebrafish. PLoS Biol. 2, E129.

Bovenkamp, D.E., Goishi, K., Bahary, N., Davidson, A.J., Zhou, Y., Becker, T., Becker, C.G., Zon, L.I., Klagsbrun, M., 2004. Expression and mapping of duplicate neuropilin-1 and neuropilin-2 genes in developing zebrafish. Gene Expression Patterns 4, 361–370.

Brown, C.B., Feiner, L., Lu, M.M., Li, J., Ma, X., Webber, A.L., Jia, L., Raper, J.A., Epstein, J.A., 2001. PlexinA2 and semaphorin signaling during cardiac neural crest development. Development 128, 3071–3080.

Chan, W.Y., Cheung, C.S., Yung, K.M., Copp, A.J., 2004. Cardiac neural crest of the mouse embryo: axial level of origin, migratory pathway and cell autonomy of the splotch (Sp2H) mutant effect. Development 131, 3367–3379.

Chen, J.N., Haffter, P., Odenthal, J., Vogelsang, E., Brand, M., van Eeden, F.J., Furutani-Seiki, M., Granato, M., Hammerschmidt, M., Heisenberg, C.P., Jiang, Y.J., Kane, D.A., Kelsh, R.N., Mullins, M.C., Nusslein-Volhard, C., 1996. Mutations affecting the cardiovascular system and other internal organs in zebrafish. Development 123, 293–302.

Draper, B.W., Morcos, P.A., Kimmel, C.B., 2001. Inhibition of zebrafish *fgf8* pre-mRNA splicing with morpholino oligos: a quantifiable method for gene knockdown. Genesis 30, 154–156.

Eickholt, B.J., Mackenzie, S.L., Graham, A., Walsh, F.S., Doherty, P., 1999. Evidence for collapsin-1 functioning in the control of neural crest migration in both trunk and hindbrain regions. Development 126, 2181–2189.

Eisenberg, L.M., Markwald, R.R., 2004. Cellular recruitment and the development of the myocardium. Dev. Biol. 274, 225–232.

Epstein, J.A., Li, J., Lang, D., Chen, F., Brown, C.B., Jin, F., Lu, M.M., Thomas, M., Liu, E., Wessels, A., Lo, C.W., 2000. Migration of cardiac neural crest cells in Splotch embryos. Development 127, 1869–1878.

Feiner, L., Webber, A.L., Brown, C.B., Lu, M.M., Jia, L., Feinstein, P., Mombaerts, P., Epstein, J.A., Raper, J.A., 2001. Targeted disruption of semaphorin 3C leads to persistent truncus arteriosus and aortic arch interruption. Development 128, 3061–3070.

Finkelstein, S.D., Dhir, R., Rabinovitz, M., Bischeglia, M., Swalsky, P.A., DeFlavia, P., Woods, J., Bakker, A., Becich, M., 1999. Cold-temperature plastic resin embedding of liver for DNA- and RNA-based genotyping. J. Mol. Diagn. 1, 17–22.

Glickman, N.S., Yelon, D., 2002. Cardiac development in zebrafish: coordination of form and function. Semin. Cell Dev. Biol. 13, 507–513.

Halloran, M.C., Berndt, J.D., 2003. Current progress in neural crest cell motility and migration and future prospects for the zebrafish model system. Dev. Dyn. 228, 497–513.

Halloran, M.C., Severance, S.M., Yee, C.S., Gemza, D.L., Raper, J.A., Kuwada, J.Y., 1999. Analysis of a Zebrafish semaphorin reveals potential functions in vivo. Dev. Dyn. 214, 13–25.

Harvey, R.P., 2002. Patterning the vertebrate heart. Nat. Rev., Genet. 3, 544–556.

Hilger-Eversheim, K., Moser, M., Schorle, H., Buettner, R., 2000. Regulatory roles of AP-2 transcription factors in vertebrate development, apoptosis and cell-cycle control. Gene 260, 1–12.

Hove, J.R., Koster, R.W., Forouhar, A.S., Acevedo-Bolton, G., Fraser, S.E., Gharib, M., 2003. Intracardiac fluid forces are an essential epigenetic factor for embryonic cardiogenesis. Nature 421, 172–177.

Huang, C.J., Tu, C.T., Hsiao, C.D., Hsieh, F.J., Tsai, H.J., 2003. Germ-line transmission of a myocardium-specific GFP transgene reveals critical regulatory elements in the cardiac myosin light chain 2 promoter of zebrafish. Dev. Dyn. 228, 30–40.

Keegan, B.R., Feldman, J.L., Begemann, G., Ingham, P.W., Yelon, D., 2005. Reti- noic acid signaling restricts the cardiac progenitor pool. Science 307, 247–249.

Kelly, R.G., Buckingham, M.E., 2002. The anterior heart-forming field: voyage to the arterial pole of the heart. Trends Genet. 18, 210–216.

Kelly, R.G., Brown, N.A., Buckingham, M.E., 2001. The arterial pole of the mouse heart forms from Fgf10-expressing cells in pharyngeal mesoderm. Dev. Cell 1, 435–440.

Kimmel, C.B., Warga, R.M., Schilling, T.F., 1990. Origin and organization of the zebrafish fate map. Development 108, 581–594.

Kimmel, C.B., Miller, C.T., Moens, C.B., 2001. Specification and morphogenesis of the zebrafish larval head skeleton. Dev. Biol. 233, 239–257.

Kirby, M.L., Waldo, K.L., 1990. Role of neural crest in congenital heart disease. Circulation 82, 332–340.

Kirby, M.L., Waldo, K.L., 1995. Neural crest and cardiovascular patterning. Circ. Res. 77, 211–215.

Kolodkin, A.L., Matthes, D.J., Goodman, C.S., 1993. The semaphorin genes encode a family of transmembrane and secreted growth cone guidance molecules. Cell 75, 1389–1399.

Lee, P., Goishi, K., Davidson, A.J., Mannix, R., Zon, L., Klagsbrun, M., 2002. Neuropilin-1 is required for vascular development and is a mediator of VEGF-dependent angiogenesis in zebrafish. Proc. Natl. Acad. Sci. U. S. A. 99 (s).

Li, Y.X., Zdanowicz, M., Young, L., Kumiski, D., Leatherbury, L., Kirby, M.L., 2003. Cardiac neural crest in zebrafish embryos contributes to myocardial cell lineage and early heart function. Dev. Dyn. 226, 540–550.

Liu, Y., Berndt, J., Su, F., Tawarayama, H., Shoji, W., Kuwada, J.Y., Halloran, M.C., 2004. Semaphorin3D guides retinal axons along the dorsoventral axis of the tectum. J. Neurosci. 24, 310–318.

Luo, Y., Raible, D., Raper, J.A., 1993. Collapsin: a protein in brain that induces the collapse and paralysis of neuronal growth cones. Cell 75, 217–227.

Luo, Y., Shepherd, I., Li, J., Renzi, M.J., Chang, S., Raper, J.A., 1995. A family of molecules related to collapsin in the embryonic chick nervous system. Neuron 14, 1131–1140.

Mark, M.D., Lohrum, M., Puschel, A.W., 1997. Patterning neuronal connections by chemorepulsion: the semaphorins. Cell Tissue Res. 290, 299–306.

Miller, C.T., Schilling, T.F., Lee, K., Parker, J., Kimmel, C.B., 2000. Sucker encodes a zebrafish Endothelin-1 required for ventral pharyngeal arch development. Development 127, 3815–3828.

Mjaatvedt, C.H., Nakaoka, T., Moreno-Rodriguez, R., Norris, R.A., Kern, M. J., Eisenberg, C.A., Turner, D., Markwald, R.R., 2001. The outflow tract of the heart is recruited from a novel heart-forming field. Dev. Biol. 238, 97–109.

Neuhauss, S.C., Solnica-Krezel, L., Schier, A.F., Zwartkruis, F., Stemple, D.L., Malicki, J., Abdelilah, S., Stainier, D.Y., Driever, W., 1996. Mutations affecting craniofacial development in zebrafish. Development 123, 357–367.

Odenthal, J., Nusslein-Volhard, C., 1998. Fork head domain genes in zebrafish. Dev. Genes Evol. 208, 245–258.

Osborne, N.J., Begbie, J., Chilton, J.K., Schmidt, H., Eickholt, B.J., 2005. Semaphorin/neuropilin signaling influences the positioning of migratory neural crest cells within the hindbrain region of the chick. Dev. Dyn. 232, 939–949.

Raper, J.A., 2000. Semaphorins and their receptors in vertebrates and invertebrates. Curr. Opin. Neurobiol. 10, 88–94.

Reiter, J.F., Alexander, J., Rodaway, A., Yelon, D., Patient, R., Holder, N., Stainier, D.Y., 1999. Gata5 is required for the development of the heart and endoderm in zebrafish. Genes Dev. 13, 2983–2995.

Rubinstein, A.L., Lee, D., Luo, R., Henion, P.D., Halpern, M.E., 2000. Genes dependent on zebrafish cyclops function identified by AFLP differential gene expression screen. Genesis 26, 86–97.

Sato, M., Yost, H.J., 2003. Cardiac neural crest contributes to cardiomyogenesis in zebrafish. Dev. Biol. 257, 127–139.

Schilling, T.F., Kimmel, C.B., 1994. Segment and cell type lineage restrictions during pharyngeal arch development in the zebrafish embryo. Development 120, 483–494.

Shu, X., Cheng, K., Patel, N., Chen, F., Joseph, E., Tsai, H.J., Chen, J.N., 2003. Na,K-ATPase is essential for embryonic heart development in the zebrafish. Development 130, 6165–6173.

Stainier, D.Y., 2001. Zebrafish genetics and vertebrate heart formation. Nat. Rev., Genet. 2, 39–48.

Stainier, D.Y., Lee, R.K., Fishman, M.C., 1993. Cardiovascular development in the zebrafish. I. Myocardial fate map and heart tube formation. Development 119, 31–40.

Stainier, D.Y., Fouquet, B., Chen, J.N., Warren, K.S., Weinstein, B.M., Meiler, S.E., Mohideen, M.A., Neuhauss, S.C., Solnica-Krezel, L., Schier, A.F., Zwartkruis, F., Stemple, D.L., Malicki, J., Driever, W., Fishman, M.C., 1996. Mutations affecting the formation and function of the cardiovascular system in the zebrafish embryo. Development 123, 285–292.

Trinh, L.A., Stainier, D.Y., 2004. Fibronectin regulates epithelial organization during myocardial migration in zebrafish. Dev. Cell 6, 371–382.

Waldo, K.L., Kumiski, D.H., Wallis, K.T., Stadt, H.A., Hutson, M.R., Platt, D.H., Kirby, M.L., 2001. Conotruncal myocardium arises from a secondary heart field. Development 128, 3179–3188.

Westerfield, M., 1994. The Zebrafish Book: A Guide for the Laboratory Use of Zebrafish (*Brachydanio rerio*). Univ. of Oregon Press, Eugene.

Willett, C.E., Zapata, A.G., Hopkins, N., Steiner, L.A., 1997. Expression of zebrafish rag genes during early development identifies the thymus. Dev. Biol. 182, 331–341.

Wolman, M.A., Liu, Y., Tawarayama, H., Shoji, W., Halloran, M.C., 2004. Repulsion and attraction of axons by Semaphorin3D are mediated by different neuropilins in vivo. J. Neurosci. 24, 8428–8435.

Yelon, D., Stainier, D.Y., 2002. Pattern formation: swimming in retinoic Acid. Curr. Biol. 12, R707–R709.

Yelon, D., Horne, S.A., Stainier, D.Y., 1999. Restricted expression of cardiac myosin genes reveals regulated aspects of heart tube assembly in zebrafish. Dev. Biol. 214, 23–37.

Yu, H.H., Moens, C.B., 2005. Semaphorin signaling guides cranial neural crest cell migration in zebrafish. Dev. Biol. 280, 373–385.

Yu, H.H., Houart, C., Moens, C.B., 2004. Cloning and embryonic expression of zebrafish neuropilin genes. Gene Expression Patterns 4, 371–378.